

Centrality dependence of dilepton production and the Wigner distributions of photons in nuclei

Wolfgang Schäfer ¹

¹ Institute of Nuclear Physics, Polish Academy of Sciences, Kraków

Lund Science Coffee, 14.6. 2022

Peripheral/ultraperipheral collisions

- Weizsäcker-Williams equivalent photons
- a part of the partonic structure of charged particles

From ultraperipheral to semicentral collisions

- dileptons from $\gamma\gamma$ production vs thermal dileptons from plasma phase
- Wigner function generalization of the Weizsäcker-Williams approach



M. Kłusek-Gawenda, R. Rapp, W. S. and A. Szczurek, “Dilepton Radiation in Heavy-Ion Collisions at Small Transverse Momentum,” Phys. Lett. B **790** (2019) 339 [arXiv:1809.07049 [nucl-th]].



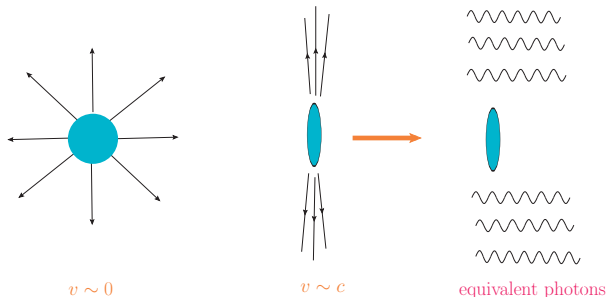
M. Kłusek-Gawenda, W. S. and A. Szczurek, “Centrality dependence of dilepton production via $\gamma\gamma$ processes from Wigner distributions of photons in nuclei,” Phys. Lett. B **814** (2021), 136114 [arXiv:2012.11973 [hep-ph]].



M. Łuszczak, W. S. and A. Szczurek, “Two-photon dilepton production in proton-proton collisions: two alternative approaches,” Phys. Rev. D **93** (2016) no.7, 074018 [arXiv:1510.00294 [hep-ph]].

Fermi-Weizsäcker-Williams equivalent photons

Heavy nuclei Au, Pb have $Z \sim 80$



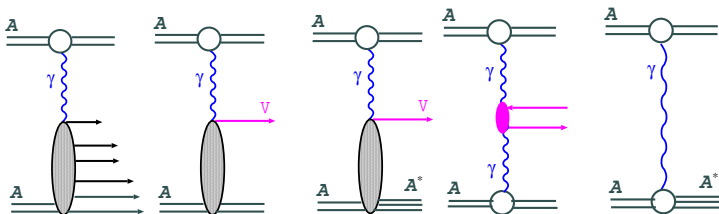
- ion at rest: source of a Coulomb field, the highly boosted ion: sharp burst of field strength, with $|\mathbf{E}|^2 \sim |\mathbf{B}|^2$ and $\mathbf{E} \cdot \mathbf{B} \sim 0$. (See e.g. J.D Jackson textbook).
- acts like a flux of “equivalent photons” (photons are collinear partons).

$$\mathbf{E}(\omega, \mathbf{b}) = -i \frac{Z\sqrt{4\pi\alpha_{em}}}{2\pi} \frac{\mathbf{b}}{b^2} \frac{\omega b}{\gamma} K_1\left(\frac{\omega b}{\gamma}\right); N(\omega, \mathbf{b}) \propto \frac{1}{\omega} |\mathbf{E}(\omega, \mathbf{b})|^2$$

$$\sigma(AB) = \int d\omega d^2\mathbf{b} N(\omega, \mathbf{b}) \sigma(\gamma B; \omega)$$

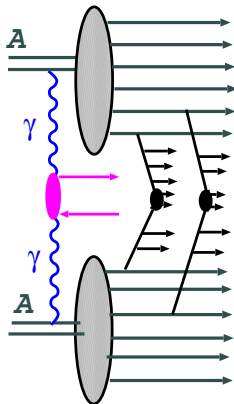
Ultrapерipheral collisions

some examples of ultraperipheral processes:



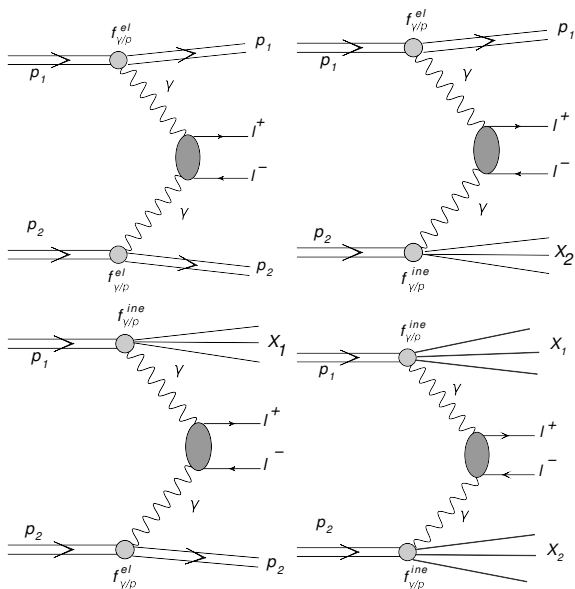
- photoabsorption on a nucleus
- diffractive photoproduction with and without breakup/excitation of a nucleus
- $\gamma\gamma$ -fusion.
- electromagnetic excitation/dissociation of nuclei. Excitation of Giant Dipole Resonances.
- the intact nuclei in the final state are not measured. Each of the photon exchanges is associated with a large rapidity gap.
- very small p_T of the photoproduced system.

Dilepton production in semi-central collisions

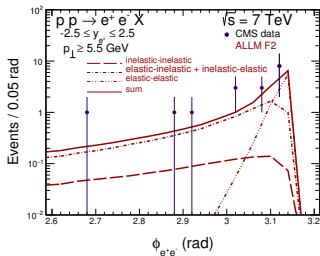
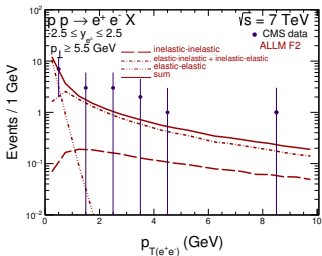


- dileptons from $\gamma\gamma$ fusion have peak at very low pair transverse momentum.
- can they be visible even in semi-central collisions?
- WW photons are a coherent “parton cloud” of nuclei, which can collide and produce particles. Nuclei create an “underlying event, in which e.g. plasma can be formed.
- Early considerations in N. Baron and G. Baur, Z. Phys. C **60** (1993).
- a first hint of the relevance of photoproduction mechanisms: a strong enhancement of J/ψ with $P_T < 300$ MeV in peripheral reactions: J. Adam *et al.* [ALICE], Phys. Rev. Lett. **116** (2016) (for early estimates, see M. Kłusek-Gawenda and A. Szczurek, Phys. Rev. C **93** (2016)).
- Dileptons are a “classic” probe of the QGP: medium modifications of ρ , thermal dileptons... What is the competition between the different mechanisms?

Dileptons from $\gamma\gamma$ -fusion in pp collisions

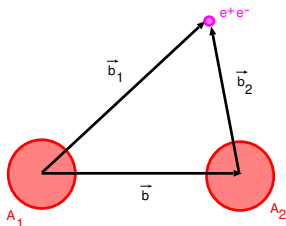


Dileptons from $\gamma\gamma$ -fusion in pp collisions



- from M. Łuszczak, W.S., A. Szczurek, Phys.Rev.D 93 (2016) 7, 074018
- “inelastic photon fluxes” correspond to the standard photon parton distributions. They can be calculated from proton structure functions F_2, F_L .
- “elastic” photon fluxes are the coherent contribution to the photon parton distribution in a proton. It can be calculated from e.m. form factors G_E, G_M .
- both are part of photon parton distributions like e.g. the k_T -factorization fluxes of ours, or e.g. LUX-QED fit.

Dilepton production in semi-central collisions



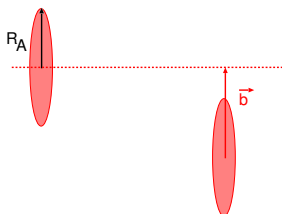
$$\frac{d\sigma_{ll}}{d\xi d^2\mathbf{b}} = \int d^2\mathbf{b}_1 d^2\mathbf{b}_2 \delta^{(2)}(\mathbf{b} - \mathbf{b}_1 - \mathbf{b}_2) N(\omega_1, b_1) N(\omega_2, b_2) \frac{d\sigma(\gamma\gamma \rightarrow l^+l^-; \hat{s})}{d(-\hat{t})},$$

where the phase space element is $d\xi = dy_+ dy_- dp_t^2$ with y_{\pm} , p_t and m_l the single-lepton rapidities, transverse momentum and mass, respectively, and

$$\omega_1 = \frac{\sqrt{p_t^2 + m_l^2}}{2} (e^{y_+} + e^{y_-}), \quad \omega_2 = \frac{\sqrt{p_t^2 + m_l^2}}{2} (e^{-y_+} + e^{-y_-}), \quad \hat{s} = 4\omega_1\omega_2.$$

- we adopt the impact parameter definition of centrality

$$\frac{dN_{ll}[C]}{dM} = \frac{1}{f_C \cdot \sigma_{AA}^{\text{in}}} \int_{b_{\text{min}}}^{b_{\text{max}}} db \int d\xi \delta(M - 2\sqrt{\omega_1\omega_2}) \left. \frac{d\sigma_{ll}}{d\xi db} \right|_{\text{cuts}},$$



- e.g. from optical limit of Glauber:

$$\frac{d\sigma_{AA}^{\text{in}}}{db} = 2\pi b(1 - e^{-\sigma_{NN}^{\text{in}} T_{AA}(b)})$$

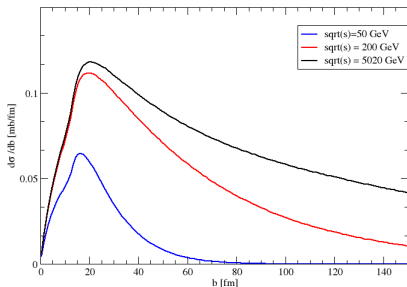
$\sigma_{AA}^{\text{in}} \sim 7$ barn for Pb at LHC.

- fraction of inelastic hadronic events contained in the centrality class \mathcal{C} ,

$$f_{\mathcal{C}} = \frac{1}{\sigma_{AA}^{\text{in}}} \int_{b_{\text{min}}}^{b_{\text{max}}} db \frac{d\sigma_{AA}^{\text{in}}}{db}.$$

- experimentally, centrality is determined by binning in multiplicity and/or transverse energy.

Dilepton production: impact parameter distribution



- semi-central collisions are situated on the left side of the distribution, below $b < 15\text{fm}$.
- starting from RHIC energies, the contribution from coherent photons is practically energy-independent.
- also notice the long tails of the ultraperipheral part. Their importance rises with energy.

Thermal dilepton production

- The calculation of thermal dilepton production from a near-equilibrated medium follows the approach of R. Rapp and E. V. Shuryak, Phys. Lett. B **473** (2000); J. Ruppert, C. Gale, T. Renk, P. Lichard and J. I. Kapusta, Phys. Rev. Lett. **100** (2008). R. Rapp and H. van Hees, Phys. Lett. B **753** (2016) 586.
- To compute dilepton invariant-mass spectra an integration of the thermal emission rate over the space-time evolution of the expanding fireball is performed,

$$\frac{dN_{ll}}{dM} = \int d^4x \frac{Md^3P}{P_0} \frac{dN_{ll}}{d^4xd^4P},$$

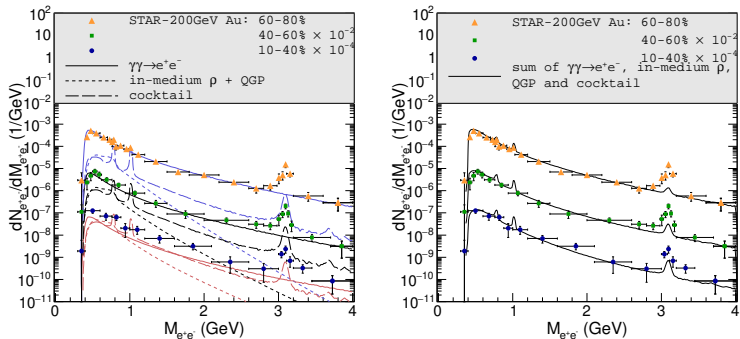
where (P_0, \vec{P}) and $M = \sqrt{P_0^2 - P^2}$ are the 4-vector ($P = |\vec{P}|$) and invariant mass of the lepton pair, respectively.

- The thermal emission rate is expressed through the EM spectral function,

$$\frac{dN_{ll}}{d^4xd^4P} = \frac{\alpha_{EM}^2 L(M)}{\pi^3 M^2} f^B(P_0; T) (-g_{\mu\nu}) \text{Im} \Pi_{EM}^{\mu\nu}(M, P; \mu_B, T),$$

- The fireball evolves through both QGP and hadronic phases. For the respective spectral functions we employ in-medium quark-antiquark annihilation and in-medium vector spectral functions in the hadronic sector.
- Different centrality classes for different colliding systems are characterized by the measured hadron multiplicities and appropriate initial conditions for the fireball.

Dilepton production in semi-central collisions



Left panel: Dielectron invariant-mass spectra for pair- $P_T < 0.15$ GeV in Au+Au ($\sqrt{s_{NN}} = 200$ GeV) collisions for 3 centrality classes including experimental acceptance cuts ($p_t > 0.2$ GeV, $|\eta_e| < 1$ and $|y_{e^+e^-}| < 1$) for $\gamma\gamma$ fusion (solid lines), thermal radiation (dotted lines) and the hadronic cocktail (dashed lines); right panel: comparison of the total sum (solid lines) to STAR data [1].

[1] data from J. Adam *et al.* [STAR Collaboration], Phys. Rev. Lett. **121** (2018) 132301.

- also added is a contribution from decays of final state hadrons "cocktail" supplied by STAR.
- the J/ψ contribution has been described e.g. in W. Zha, L. Ruan, Z. Tang, Z. Xu and S. Yang, Phys. Lett. B **789** (2019), 238-242 [arXiv:1810.02064 [hep-ph]].

Pair transverse momentum distribution

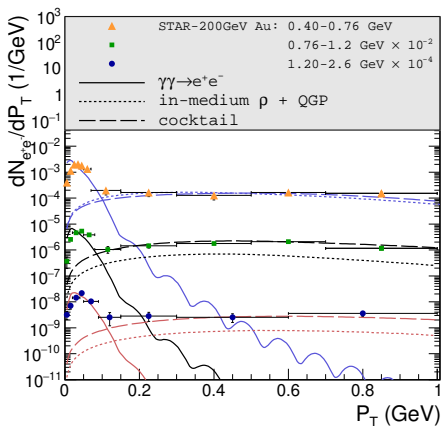
- Here we perform a simplified calculation by using b -integrated **transverse momentum dependent photon fluxes**,

$$\frac{dN(\omega, q_t^2)}{d^2\vec{q}_t} = \frac{Z^2\alpha_{EM}}{\pi^2} \frac{q_t^2}{[q_t^2 + \frac{\omega^2}{\gamma^2}]^2} F_{\text{em}}^2(q_t^2 + \frac{\omega^2}{\gamma^2}).$$

$$\frac{d\sigma_{\parallel}}{d^2\vec{P}_T} = \int \frac{d\omega_1}{\omega_1} \frac{d\omega_2}{\omega_2} d^2\vec{q}_{1t} d^2\vec{q}_{2t} \frac{dN(\omega_1, q_{1t}^2)}{d^2\vec{q}_{1t}} \frac{dN(\omega_2, q_{2t}^2)}{d^2\vec{q}_{2t}} \delta^{(2)}(\vec{q}_{1t} + \vec{q}_{2t} - \vec{P}_T) \hat{\sigma}(\gamma\gamma \rightarrow l^+l^-) \Big|_{\text{cuts}}$$

- analogous to **TMD-factorization** in hard processes. Note that experiment includes a cut $p_t(\text{lepton}) > 0.2 \text{ GeV}$. Formfactors ensure that photon virtualities are much smaller than this “hard scale”. We can thus treat them as **on-shell** in the $\gamma\gamma \rightarrow e^+e^-$ cross section.
- notice the extremely sharp peak in q_t , which is cut off only by ω/γ . The peak will move towards smaller q_t as the boost γ increases.

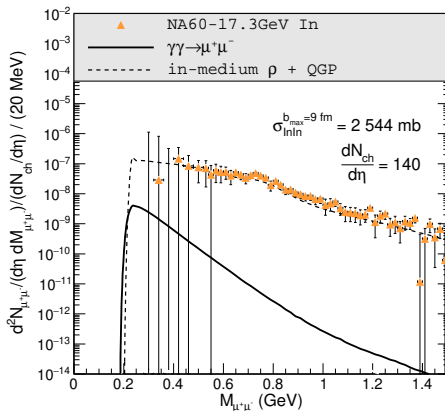
Dilepton production in semi-central collisions



P_T spectra of the individual contributions (line styles as in the previous figure) in 3 different mass bins for 60-80% central Au+Au collisions ($\sqrt{s_{NN}}=200$ GeV), compared to STAR data [1].

[1] J. Adam *et al.* [STAR Collaboration], Phys. Rev. Lett. **121** (2018) 132301.

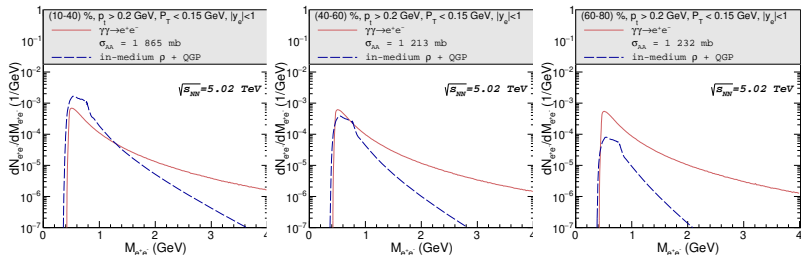
Dilepton production in semi-central collisions



Low- P_T ($<0.2 \text{ GeV}$) acceptance-corrected dimuon invariant mass excess spectra in the rapidity range $3.3 < Y_{\mu^+\mu^-, LAB} < 4.2$ for MB In+In ($\sqrt{s_{NN}}=17.3 \text{ GeV}$) collisions at the SPS. Calculations for coherent $\gamma\gamma$ fusion (solid line) and thermal radiation (dashed line) are compared to NA60 data [1].

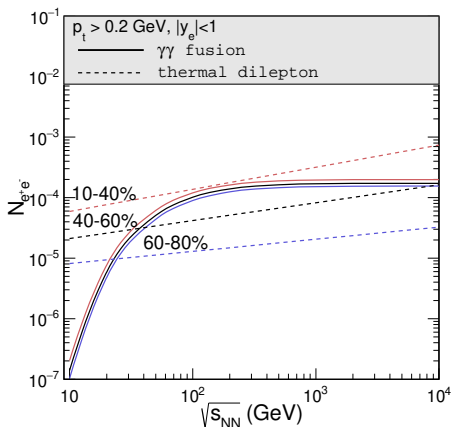
[1] R. Arnaldi *et al.* [NA60 Collaboration], *Eur. Phys. J. C* **61** (2009) 711.

Dilepton production in semi-central collisions



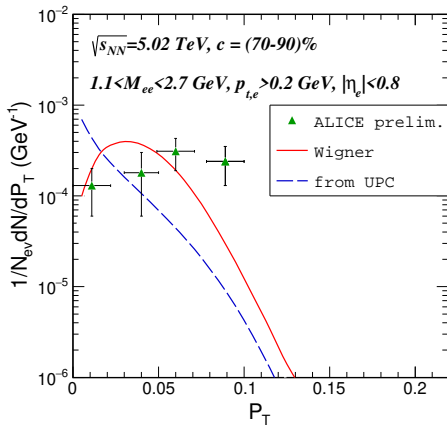
Our predictions for low- P_T dilepton radiation in Pb+Pb ($\sqrt{s_{NN}}=5.02$ TeV) collisions from coherent $\gamma\gamma$ fusion (solid lines) and thermal radiation (dashed lines) for three centrality classes and acceptance cuts as specified in the figures.

Dilepton production in semi-central collisions



Excitation function of low- P_T ($< 0.15 \text{ GeV}$) dilepton yields from $\gamma\gamma$ fusion (solid lines) and thermal radiation (dashed lines) in collisions of heavy nuclei ($A \simeq 200$) around midrapidity in three centrality classes, including single- e^\pm acceptance cuts.

P_T -distribution of the pair at LHC energies



P_T distribution of the pair against ALICE data.

Wigner function approach

- We need to find a generalization of photon fluxes (or parton distributions), that contain information on both impact parameter and transverse momentum. This is achieved by the **Wigner function**.
- We also have to take into account photon polarizations, so in fact we obtain a density matrix of Wigner functions:

$$N_{ij}(\omega, \mathbf{b}, \mathbf{q}) = \int \frac{d^2 \mathbf{Q}}{(2\pi)^2} \exp[-i\mathbf{b}\mathbf{Q}] E_i\left(\omega, \mathbf{q} + \frac{\mathbf{Q}}{2}\right) E_j^*\left(\omega, \mathbf{q} - \frac{\mathbf{Q}}{2}\right)$$

- when summed over polarizations it reduces to the well-known WW flux after integrating over \mathbf{q} , and to the TMD photon flux after integrating over \mathbf{b} :

$$N(\omega, \mathbf{q}) = \delta_{ij} \int d^2 \mathbf{b} N_{ij}(\omega, \mathbf{b}, \mathbf{q}) = \delta_{ij} E_i(\omega, \mathbf{q}) E_j^*(\omega, \mathbf{q}) = \left| \mathbf{E}(\omega, \mathbf{q}) \right|^2,$$

$$N(\omega, \mathbf{b}) = \delta_{ij} \int \frac{d^2 \mathbf{q}}{(2\pi)^2} N_{ij}(\omega, \mathbf{b}, \mathbf{q}) = \delta_{ij} E_i(\omega, \mathbf{b}) E_j^*(\omega, \mathbf{b}) = \left| \mathbf{E}(\omega, \mathbf{b}) \right|^2.$$

- Field strength vector:

$$\mathbf{E}(\omega, \mathbf{q}) \propto \frac{\mathbf{q} F(q^2)}{q^2 + \frac{\omega^2}{\gamma^2}}$$

Wigner function approach

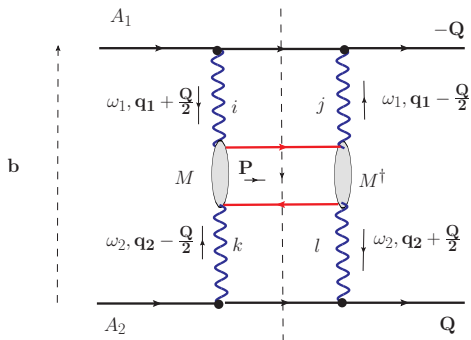
- The Wigner function is the Fourier transform of a generalized transverse momentum distribution (GTMD), and in some sense (at small- x) the most general function in the zoo of parton correlators. For the photon case, see S. Klein, A. H. Mueller, B. W. Xiao and F. Yuan, Phys. Rev. D **102** (2020) no.9, 094013.
- Recently, there has been a lot of interest in the gluon Wigner distributions, which has applications in exclusive diffractive processes. See e.g. Y. Hagiwara, Y. Hatta, R. Pasechnik, M. Tasevsky and O. Teryaev, Phys. Rev. D **96** (2017) no.3, 034009.
- In our case we have the simple factorization formula for the cross section:

$$\frac{d\sigma}{d^2\mathbf{b}d^2\mathbf{P}} = \int d^2\mathbf{b}_1 d^2\mathbf{b}_2 \delta^{(2)}(\mathbf{b} - \mathbf{b}_1 + \mathbf{b}_2) \int \frac{d\omega_1}{\omega_1} \frac{d\omega_2}{\omega_2} d^2\mathbf{q}_1 d^2\mathbf{q}_2 \delta^{(2)}(\mathbf{P} - \mathbf{q}_1 - \mathbf{q}_2) \\ \times N_{ij}(\omega_1, \mathbf{b}_1, \mathbf{q}_1) N_{kl}(\omega_2, \mathbf{b}_2, \mathbf{q}_2) \frac{1}{2\hat{s}} M_{ik} M_{jl}^\dagger d\Phi(I^+ I^-).$$

- no independent sum over photon polarizations!
- other approaches: M. Vidovic, M. Greiner, C. Best and G. Soff, Phys. Rev. **C47** (1993); K. Hencken, G. Baur and D. Trautmann, Phys. Rev. C **69** (2004) 054902; S. Klein et al. (2020).

Wigner function approach

$$\begin{aligned}
 \frac{d\sigma}{d^2b d^2P} &= \int \frac{d^2Q}{(2\pi)^2} \exp[-i\mathbf{b}Q] \int \frac{d\omega_1}{\omega_1} \frac{d\omega_2}{\omega_2} \int \frac{d^2q_1}{\pi} \frac{d^2q_2}{\pi} \delta^{(2)}(\mathbf{P} - \mathbf{q}_1 - \mathbf{q}_2) \\
 &\times E_i\left(\omega_1, \mathbf{q}_1 + \frac{\mathbf{Q}}{2}\right) E_j^*\left(\omega_1, \mathbf{q}_1 - \frac{\mathbf{Q}}{2}\right) E_k\left(\omega_2, \mathbf{q}_2 - \frac{\mathbf{Q}}{2}\right) E_l^*\left(\omega_2, \mathbf{q}_2 + \frac{\mathbf{Q}}{2}\right) \\
 &\times \frac{1}{2\hat{s}} \sum_{\lambda\bar{\lambda}} M_{ik}^{\lambda\bar{\lambda}} M_{jl}^{\lambda\bar{\lambda}\dagger} d\Phi(I^+ I^-).
 \end{aligned}$$



Wigner function approach

$$\begin{aligned}
 \frac{d\sigma}{d^2\mathbf{b}d^2\mathbf{P}} &= \int \frac{d^2\mathbf{Q}}{(2\pi)^2} \exp[-i\mathbf{bQ}] \int \frac{d\omega_1}{\omega_1} \frac{d\omega_2}{\omega_2} \int \frac{d^2\mathbf{q}_1}{\pi} \frac{d^2\mathbf{q}_2}{\pi} \delta^{(2)}(\mathbf{P} - \mathbf{q}_1 - \mathbf{q}_2) \\
 &\times E_i\left(\omega_1, \mathbf{q}_1 + \frac{\mathbf{Q}}{2}\right) E_j^*\left(\omega_1, \mathbf{q}_1 - \frac{\mathbf{Q}}{2}\right) E_k\left(\omega_2, \mathbf{q}_2 - \frac{\mathbf{Q}}{2}\right) E_l^*\left(\omega_2, \mathbf{q}_2 + \frac{\mathbf{Q}}{2}\right) \\
 &\times \frac{1}{2\hat{s}} \sum_{\lambda\bar{\lambda}} M_{ik}^{\lambda\bar{\lambda}} M_{jl}^{\lambda\bar{\lambda}\dagger} d\Phi(I^+ I^-).
 \end{aligned}$$

with

$$\begin{aligned}
 \sum_{\lambda\bar{\lambda}} M_{ik}^{\lambda\bar{\lambda}} M_{jl}^{\lambda\bar{\lambda}\dagger} &= \delta_{ik} \delta_{jl} \sum_{\lambda\bar{\lambda}} \left| M_{\lambda\bar{\lambda}}^{(0,+)} \right|^2 + \epsilon_{ik} \epsilon_{jl} \sum_{\lambda\bar{\lambda}} \left| M_{\lambda\bar{\lambda}}^{(0,-)} \right|^2 \\
 &+ P_{ik}^{\parallel} P_{jl}^{\parallel} \sum_{\lambda\bar{\lambda}} \left| M_{\lambda\bar{\lambda}}^{(2,-)} \right|^2 + P_{ik}^{\perp} P_{jl}^{\perp} \sum_{\lambda\bar{\lambda}} \left| M_{\lambda\bar{\lambda}}^{(2,+)} \right|^2
 \end{aligned}$$

$$\delta_{ik} = \hat{x}_i \hat{x}_k + \hat{y}_i \hat{y}_k, \quad \epsilon_{ik} = \hat{x}_i \hat{y}_k - \hat{y}_i \hat{x}_k, \quad P_{ik}^{\parallel} = \hat{x}_i \hat{x}_k - \hat{y}_i \hat{y}_k, \quad P_{ik}^{\perp} = \hat{x}_i \hat{y}_k + \hat{y}_i \hat{x}_k$$

- In the $\gamma\gamma$ CM, colliding photons can be in the $J_z = 0, \pm 2$ states.

Photon polarization dependence

- We have decomposed the $\gamma\gamma \rightarrow l^+l^-$ amplitude into channels of total angular momentum projection $J_z = 0, \pm 2$ and even and odd parity. The explicit expressions for the squares of amplitudes, in terms of cm-scattering angle θ read:

$$\sum_{\lambda\bar{\lambda}} \left| M_{\lambda\bar{\lambda}}^{(0,+)} \right|^2 = g_{\text{em}}^4 \frac{8(1-\beta^2)\beta^2}{(1-\beta^2\cos^2\theta)^2},$$

$$\sum_{\lambda\bar{\lambda}} \left| M_{\lambda\bar{\lambda}}^{(0,-)} \right|^2 = g_{\text{em}}^4 \frac{8(1-\beta^2)}{(1-\beta^2\cos^2\theta)^2},$$

$$\sum_{\lambda\bar{\lambda}} \left| M_{\lambda\bar{\lambda}}^{(2,+)} \right|^2 = g_{\text{em}}^4 \frac{8\beta^2\sin^2\theta}{(1-\beta^2\cos^2\theta)^2} \left(1 - \beta^2\sin^2\theta\right),$$

$$\sum_{\lambda\bar{\lambda}} \left| M_{\lambda\bar{\lambda}}^{(2,-)} \right|^2 = g_{\text{em}}^4 \frac{8\beta^2\sin^2\theta}{(1-\beta^2\cos^2\theta)^2},$$

where $g_{\text{em}}^2 = 4\pi\alpha_{\text{em}}$, and

$$\beta = \sqrt{1 - \frac{4m_l^2}{M_{l^+l^-}^2}}$$

- is the lepton velocity in the dilepton cms-frame. Notice that in the ultrarelativistic limit $\beta \rightarrow 1$, the $|J_z| = 2$ terms dominate, while for $\beta \ll 1$, relevant for heavy fermions, the $J_z = 0$ components are the leading ones (pseudoscalar channel dominates).

- Wigner function is not necessarily a non-negative function. One may doubt, whether our cross section is manifestly positive, i.e. well-defined. To this end, we can introduce:

$$G_{ik}(\omega_1, \omega_2, \mathbf{P}; \mathbf{b}) \equiv \int \frac{d^2\mathbf{k}}{2\pi^2} \exp[-i\mathbf{b}\mathbf{k}] E_i(\omega_1, \mathbf{k}) E_k(\omega_2, \mathbf{P} - \mathbf{k}),$$

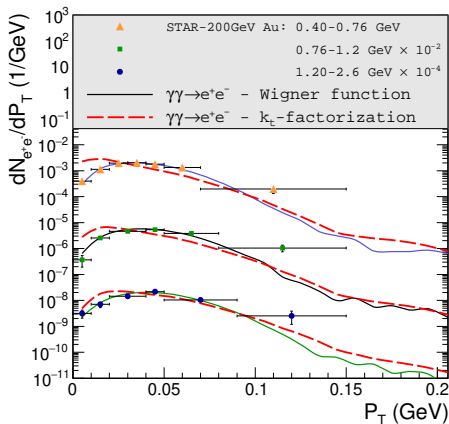
so that our cross section takes the form

$$\frac{d\sigma}{d^2\mathbf{b}d^2\mathbf{P}} = \int \frac{d\omega_1}{\omega_1} \frac{d\omega_2}{\omega_2} G_{ik}(\omega_1, \omega_2, \mathbf{P}; \mathbf{b}) G_{jl}^*(\omega_1, \omega_2, \mathbf{P}; \mathbf{b}) \frac{1}{2\hat{s}} \sum_{\lambda\bar{\lambda}} M_{ik}^{\lambda\bar{\lambda}} M_{jl}^{\lambda\bar{\lambda}\dagger} d\Phi(I^+I^-).$$

from which we obtain the cross section as a sum of squares which is manifestly positive:

$$\begin{aligned} \frac{d\sigma}{d^2\mathbf{b}d^2\mathbf{P}} = & \int \frac{d\omega_1}{\omega_1} \frac{d\omega_2}{\omega_2} \left\{ |G_{xx} + G_{yy}|^2 \sum_{\lambda\bar{\lambda}} \left| M_{\lambda\bar{\lambda}}^{(0,+)} \right|^2 + |G_{xy} - G_{yx}|^2 \sum_{\lambda\bar{\lambda}} \left| M_{\lambda\bar{\lambda}}^{(0,-)} \right|^2 \right. \\ & \left. + |G_{xx} - G_{yy}|^2 \sum_{\lambda\bar{\lambda}} \left| M_{\lambda\bar{\lambda}}^{(2,+)} \right|^2 + |G_{xy} + G_{yx}|^2 \sum_{\lambda\bar{\lambda}} \left| M_{\lambda\bar{\lambda}}^{(0,-)} \right|^2 \right\} \frac{d\Phi(I^+I^-)}{2\hat{s}}. \end{aligned}$$

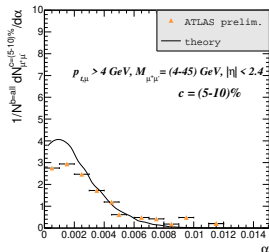
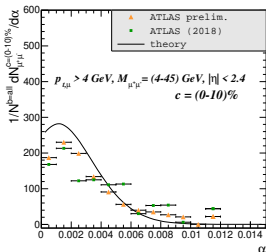
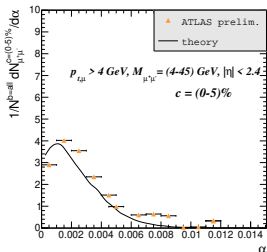
Dilepton production in semi-central collisions



P_T spectra for 60-80% central Au+Au collisions ($\sqrt{s_{NN}}=200$ GeV, 5020 GeV).

- Improved description of RHIC data in Wigner-function approach.

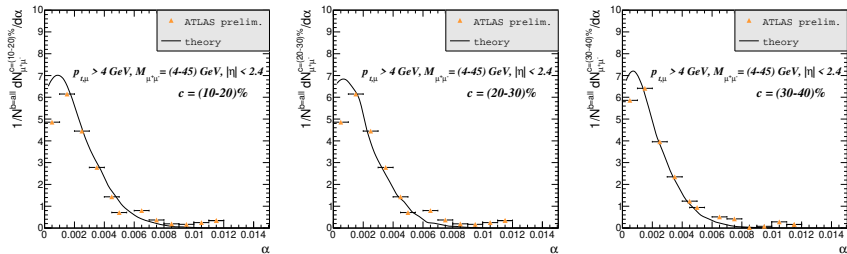
Acoplanarity distributions at LHC energies ($\sqrt{s_{NN}} = 5 \text{ TeV}$)



Data from ATLAS, ATLAS-CONF-2019-051

- acoplanarity distribution of dimuons $\alpha = 1 - \frac{\Delta\phi}{\pi}$ in different bins of centrality

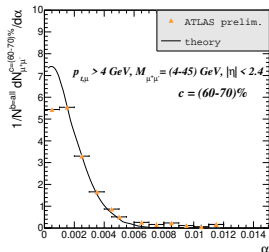
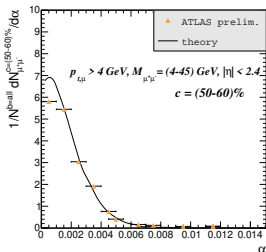
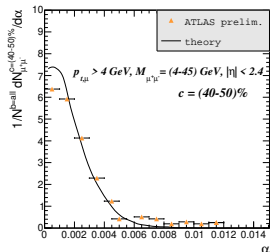
Acoplanarity distributions at LHC energies ($\sqrt{s_{NN}} = 5 \text{ TeV}$)



Data from ATLAS, ATLAS-CONF-2019-051

- acoplanarity distribution of dimuons $\alpha = 1 - \frac{\Delta\phi}{\pi}$ in different bins of centrality

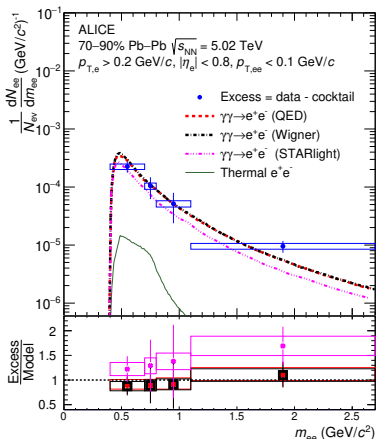
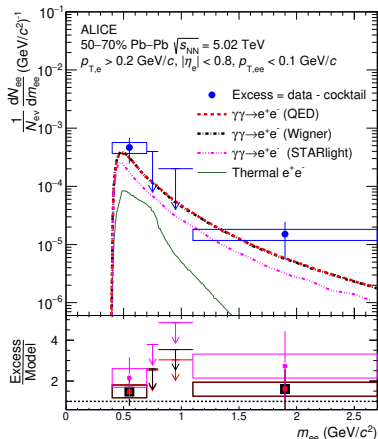
Acoplanarity distributions at LHC energies ($\sqrt{s_{NN}} = 5 \text{ TeV}$)



Data from ATLAS, ATLAS-CONF-2019-051

- acoplanarity distribution of dimuons $\alpha = 1 - \frac{\Delta\phi}{\pi}$ in different bins of centrality

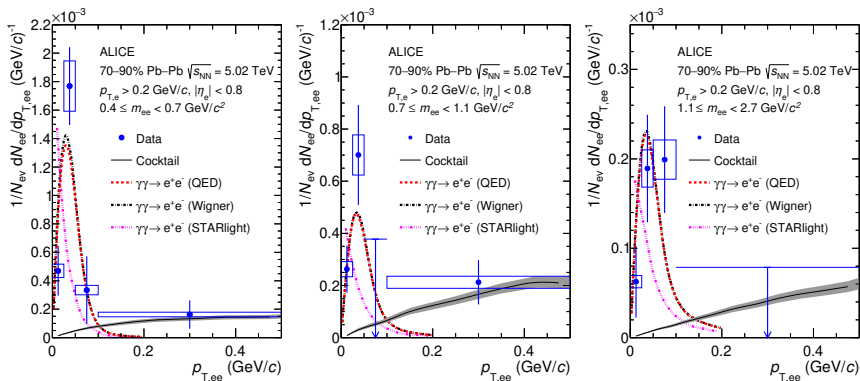
Our predictions against ALICE data: invariant mass



Data from ALICE, [arXiv:2204.11732 [nucl-ex]].

- our results: “Wigner”, M. Kłusek-Gawenda, W. S. and A. Szczurek, Phys. Lett. B **814** (2021), 136114.
- also shown are the results of the STARLIGHT MC, as well as calculations by W. Zha, J. D. Brandenburg, Z. Tang and Z. Xu, Phys.Lett.B 800 (2020) 135089, Eur.Phys.J.A 57 (2021) 10, 299.

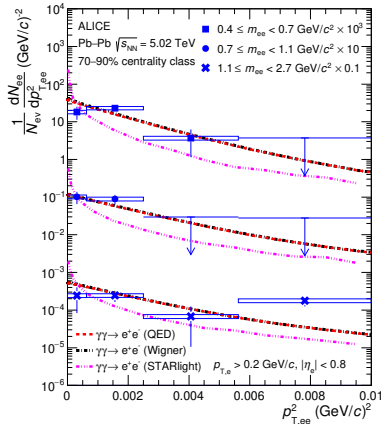
Our predictions against ALICE data: pair P_T



Data from ALICE, ‘Dielectron production at midrapidity at low transverse momentum in peripheral and semi-peripheral Pb–Pb collisions at $\sqrt{s_{NN}} = 5.02$ TeV,’ [arXiv:2204.11732 [nucl-ex]].

- our results: “Wigner”, M. Kłusek-Gawenda, W. S. and A. Szczurek, Phys. Lett. B **814** (2021), 136114.
- also shown are the results of the STARLIGHT MC, as well as calculations by W. Zha, J. D. Brandenburg, Z. Tang and Z. Xu, Phys.Lett.B 800 (2020) 135089, Eur.Phys.J.A 57 (2021) 10, 299.
- detector resolution effects are included.

Our predictions against ALICE data: pair P_T



ALICE [arXiv:2204.11732 [nucl-ex]].

$\sqrt{\langle p_{T,ee}^2 \rangle}$

Mass range (GeV)	Wigner	STARLIGHT	ALICE data
$0.4 \leq M \leq 0.7$	45 MeV	30 MeV	44 ± 28 (stat.) ± 6 (syst.) MeV
$0.7 \leq M \leq 1.1$	48 MeV	38 MeV	45 ± 36 (stat.) ± 8 (syst.) MeV
$1.1 \leq M \leq 2.7$	50 MeV	42 MeV	69 ± 36 (stat.) ± 8 (syst.) MeV

Summary

- We have studied low- P_T dilepton production in ultrarelativistic heavy-ion collisions, by a systematic comparisons of **thermal radiation** and **photon-photon fusion** within the coherent fields of the incoming nuclei.
- Comparison to recent **STAR data**: good description of low- P_T dilepton data in Au-Au($\sqrt{s_{NN}}=200$ GeV) collisions in three centrality classes, for invariant masses from threshold to ~ 4 GeV.
- Coherent emission dominant for the two peripheral samples, and comparable to the cocktail and thermal radiation yields in semi-central collisions.
- At SPS energies ($\sqrt{s_{NN}}=17.3$ GeV) we found that the $\gamma\gamma$ contribution is subleading. Only relevant at low P_T and near the dimuon threshold, rapidly falling off with increasing mass.
- Impact-parameter dependent dilepton P_T distribution is described by a **Wigner function density matrix generalization of the Weizsäcker-Williams fluxes**. Different weights of $J_z = 0, \pm 2$ channels of the $\gamma\gamma$ -system. For e^+e^- pairs the $J_z = \pm 2$ channels dominate.
- We obtain an improved description of RHIC data.
- Proper account for the b -dependence is crucial at LHC energies.
- We obtain a very good description of ATLAS azimuthal decorrelations, our predictions agree well with recent ALICE data.
- There appears to be no clear sign of a conjectured broadening of dilepton distributions from rescattering in (the magnetic field of) the plasma.